A X-linked nonsense APOO/MIC26 variant causes a lethal mitochondrial disease with progeria-like phenotypes

Leon Peifer-Weiß, Mazen Kurban, Céline David, Melissa Lubeck, Arun Kumar Kondadi, Georges Nemer, Andreas S. Reichert, Ruchika Anand

Received: 13 June 2023 | Revised: 16 August 2023 | Accepted: 18 August 2023

DOI: 10.1111/cge.14420

ORIGINAL ARTICLE

CLINICAL GENETICS WILEY

A X-linked nonsense *APOO/MIC26* variant causes a lethal mitochondrial disease with progeria-like phenotypes

Leon Peifer-Weiß[1] | Mazen Kurban[2,3] | Céline David[1] | Melissa Lubeck[1] | Arun Kumar Kondadi[1] | Georges Nemer[4] | Andreas S. Reichert[1] | Ruchika Anand[1]

[1]Institute of Biochemistry and Molecular Biology I, Medical Faculty and University Hospital Düsseldorf, Heinrich Heine University Düsseldorf, Düsseldorf, Germany

[2]Department Biochemistry and Molecular Genetics, American University of Beirut, Beirut, Lebanon

[3]Department of Dermatology, American University of Beirut, Beirut, Lebanon

[4]College of Health and Life Sciences, Hamad Bin Khalifa University, Doha, Qatar

Correspondence
Georges Nemer, College of Health and Life Sciences, Hamad Bin Khalifa University, Education City, Doha, Qatar.
Email: gnemer@hbku.edu.qa

Ruchika Anand, Institute of Biochemistry and Molecular Biology I, Medical Faculty and University Hospital Düsseldorf, Heinrich Heine University Düsseldorf, Düsseldorf, Germany.
Email: anand@hhu.de

Present address
Leon Peifer-Weiß, Institute for Clinical Biochemistry and Pathobiochemistry, German Diabetes Center, Leibniz-Center for Diabetes Research at Heinrich Heine University, Düsseldorf, Germany.

Funding information
Deutsche Forschungsgemeinschaft, Grant/Award Numbers: AN 1440/3-1, AN 1440/4-1, KO 6519/1-1, GRK 2576 Vivid; Medizinische Fakultät, Heinrich-Heine-Universität Düsseldorf, Grant/Award Numbers: Foko-02/2015, FoKo-2020-71

Abstract

APOO/MIC26 is a subunit of the MICOS complex required for mitochondrial cristae morphology and function. Here, we report a novel variant of the *APOO/MIC26* gene that causes a severe mitochondrial disease with overall progeria-like phenotypes in two patients. Both patients developed partial agenesis of the corpus callosum, bilateral congenital cataract, hypothyroidism, and severe immune deficiencies. The patients died at an early age of 12 or 18 months. Exome sequencing revealed a mutation (NM_024122.5): c.532G>T (p.E178*) in the *APOO/MIC26* gene that causes a nonsense mutation leading to the loss of 20 C-terminal amino acids. This mutation resulted in a highly unstable and degradation prone MIC26 protein, yet the remaining minute amounts of mutant MIC26 correctly localized to mitochondria and interacted physically with other MICOS subunits. *MIC26* KO cells expressing MIC26 harboring the respective *APOO/MIC26* mutation showed mitochondria with perturbed cristae architecture and fragmented morphology resembling *MIC26* KO cells. We conclude that the novel mutation found in the *APOO/MIC26* gene is a loss-of-function mutation impairing mitochondrial morphology and cristae morphogenesis.

KEYWORDS
apolipoproteins, congenital disorder, mitochondria, mitochondrial disease, progeria

Leon Peifer-Weiß and Mazen Kurban shared first authors.

1 | INTRODUCTION

Mitochondria are vital cellular organelles as they perform many important cellular functions such as energy conversion, calcium homeostasis, programmed cell death, heme synthesis, cellular signaling, and metabolic processes. Endosymbiotic in origin, mitochondria contain their own genome (mtDNA) and encode few yet essential components required for oxidative phosphorylation and ATP production. All other mitochondrial proteins are encoded by the nuclear genome and therefore the functioning of many mitochondrial protein complexes including respiratory chain complexes (RCCs) rely on an intricate balance between assembly of the mtDNA-encoded and nuclear-encoded components. Genetic disorders in either nuclear-encoded or mtDNA genes can lead to set of diseases called mitochondrial diseases.[1] These are described as multisystemic diseases as many organs like brain, skeletal muscles, heart, liver, and kidney could be affected. No cure is available for mitochondrial diseases, which have a prevalence greater than 1.6 in 5000.[2]

The ultrastructure of the mitochondria is highly organized and contain two membranes, outer membrane (OM) and inner membrane (IM). Although the OM surrounds the mitochondria, the IM is located within and has many folds called cristae. The cristae membrane is compositionally distinct from the inner boundary membrane (IBM), a part of IM that runs parallel to OM.[3,4] RCCs are enriched in cristae and therefore cristae are the main energy producing spatial domains within mitochondria.[5] Cristae are connected to IBM by narrow openings called crista junctions (CJs).[6] CJs are highly conserved structures of very small diameter and thus limit the access of proteins and metabolites from the cristae lumen to the intermembrane space (IMS) or vice versa.[7] Recent advances in super-resolution imaging techniques show that cristae are dynamic entities,[8–12] that can constantly undergo cycles of putative fusion and fission.[13] The physiological benefits of these fast cristae dynamics on mitochondrial functions are not yet identified. A highly conserved protein complex called "mitochondrial contact site and cristae organizing system" (MICOS) is enriched at the CJs which maintains cristae structure and stabilizes CJs.[14–17] Mammalian MICOS complex contains seven bona fide subunits, IMMT/MIC60, CHCHD3/MIC19, CHCHD6/MIC25, MICOS10/MIC10, MICOS13/MIC13, APOO/MIC26, and APOOL/MIC27, which are organized into two smaller subcomplexes, MIC60-subcomplex (MIC60-19-25), and MIC10-subcomplex (MIC10-MIC13-MIC26-MIC27). MIC13 functions as a bridge between two subcomplexes[18,19] via its conserved GxxxG and WN motifs.[20] MIC60 and MIC10 are considered as the core subunits of MICOS complex because their deficiencies show severe cristae defects.[21] They both possess membrane bending activities.[22–24] Structural studies show that MIC60 forms bow-shaped tetrameric assemblies that are promoted by MIC19. This MIC60-MIC19 complex can transvers CJs and help in controlling CJ architecture.[25] The MIC60-subcomplex mainly interacts with OM proteins namely SAMM50 and Metaxins to form a larger "mitochondrial intermembrane space bridging" (MIB) complex that spans the IM and OM and helps in formation of contact sites between them.[26,27] Apart from their role in cristae organization, MICOS proteins participate in many other mitochondrial functions, including respiration, protein import, lipid transport, mtDNA organization, apoptosis, inflammation, and autophagy.[28–32]

APOO/MIC26 and APOOL/MIC27 belong to apolipoprotein family due to the presence of a conserved apolipoprotein domain. MIC26 was first identified at elevated levels in the cardiac transcriptome of high-fat diet fed dogs.[33] The protein levels of MIC26 were increased in plasma of patients with acute coronary syndrome.[34] *MIC26* deficiency in mouse adipocytes leads to aggravated brown adipose tissue whitening and diet-induced obesity indicating its role in regulating lipid metabolism.[35] Downregulation of *MIC26* shows differential expression of genes involved in fatty acid metabolism and inflammatory responses.[36] It was believed that MIC26 gets O-glycosylated and accumulates as a 55 KDa secreted protein. Later MIC26 was shown to be mitochondrially localized[37] and identified as a subunit of MICOS complex.[38] However, it was inconsistent that the recombinant MIC26 resulted in only 22 KDa band and there were discrepancies about the significance of the 55 KDa secreted form. We recently showed that MIC26 and MIC27 are exclusively mitochondrial localized as bona fide subunits of the MICOS complex and that MIC26 does not exist as a glycosylated form by using a combination of siRNAs and knockout (KO) of *MIC26* and *MIC27* in four different human cell lines and four anti-MIC26 antibodies. The 55 KDa band was present even in the KO of *MIC26* and mass spectrometry of 55 KDa protein did not contain any MIC26-specific peptides, showing that the 55 KDa band was non-specific.[39]

MIC26 and MIC27 show antagonistic regulation at the protein level where a decrease in the levels of one of them leads to an increase in protein levels of another and vice versa.[38] Although they are not considered as core components of MICOS complex, the double KO of *MIC26* and *MIC27* shows drastic loss of CJs. MIC26 and MIC27 cooperate to regulate the stability and integrity of the RCCs and the F_1F_O ATP synthase.[40] MIC27 binds cardiolipin[41] and both MIC26 and MIC27 cooperatively regulate the levels of cardiolipin in mitochondria.[40] In yeast, Mic26-Mic27 antagonism regulates the assembly of Mic10.[42] A mutation in transmembrane domain of *APOO/MIC26* was associated with mitochondrial myopathy, lactic acidosis, cognitive impairment, and autistic features.[43] Here, we report a novel variant of *MIC26* which was found in siblings from Lebanon. Unlike the other reported *MIC26* variant,[43] this variant is very severe and causes a lethal mitochondrial disease with progeria-like phenotypes.

2 | MATERIALS AND METHODS

2.1 | Patients recruitment and DNA samples

The recruitment of the family was conducted at the Genodermatoses' unit at the Department of Dermatology at the American University of Beirut Medical Center (AUBMC, Beirut, Lebanon). The clinical phenotypes were provided by the referring physician, and the project received approval from the Institutional Review Board at the American University of Beirut Medical Center. Written informed consent was obtained from the parents. Peripheral blood samples were collected from the participating individuals and stored at 4°C. Within 1 h of blood collection, DNA was extracted from the specimens and stored at 4°C.

2.2 | Whole exome sequencing

Whole Exome Sequencing (Huffmeier et al) was performed by Macrogen Laboratory in Seoul, South Korea. The sequencing was carried out using the Illumina NovaSeq6000 platform, generating 101 base pair (pair-ended) reads. The library preparation followed the manufacturer's protocol, involving random fragmentation of the DNA, adapter ligation, tagmentation, PCR amplification, gel purification, and loading the library into a flow cell. The fragments were captured on a lawn of surface-bound oligos for cluster generation, and each fragment was amplified using bridge amplification into distinctive, clonal clusters.

2.3 | Sequence analysis

The base calling of the captured raw images was performed using the RTA (Real Time Analysis) software. The BCL (base calls) binary data was converted into FASTQ (paired-end reads) using the Illumina package bcl2fastq. Quality control checks were conducted, ensuring a Phred score of approximately 33. The FASTQ files were then mapped to the Human GRCh37/hg19 reference assembly using CLC Genomics Workbench (version 20.0.4). Failed and broken reads were removed, and a minimum coverage of 10 reads and a minimum variant allele frequency of 35% were applied. The basic variant parameter ploidy was set at 2, and reference masking positions with coverage above 100,000 were ignored. CLC Genomics Workbench generated Binary Alignments Map (BAM) and Variant Call Format (VCF) files for each sample, including all the variants.

2.4 | Variant calling and annotation

The VCF files were uploaded to Illumina Variant Studio 3.0 for variant calling and annotation. The annotation was based on dbSNP, ClinVar, and the 1000 Genomes project. To identify mutations/variants potentially associated with the diseases, a stringent filter was applied using CLC Genomics and various in silico prediction tools. The criteria for filtering included: (1) novel/rare variants with minor allele frequency (MAF) <5% and read depth >20, conserved based on Genome Aggregation Database (gnomAD) ExAC, 1000 genomes, more than 300 Lebanese in-house exomes, and PhastCons and PhyloP-conservation scores; (2) functionality, pathogenicity, and protein effect predicted to be deleterious/pathogenic by PolyPhen/SIFT, American College of Medical Genetics and Genomics (ACMG) classification, mutation taster, and combined annotation dependent depletion (CADD) scores; (3) single nucleotide variants (SNVs), insertions, and deletions, including mutation types like nonsense, missense, frame shift, and splice; (4) genomic position; and (5) homozygous/heterozygous state determined by uploading BAM files to the integrative genomics viewer (IGV), a high-performance visualization tool for genomic annotations and correct calling.

The details of other materials and methods are included in Data S1.

3 | RESULTS

3.1 | Clinical presentation of patient 1

Patient 1 was first-born boy born in a non-consanguineous marriage of Lebanese parents (Figure 1A). Both the parents are healthy with no phenotypes in families on both sides. There was intrauterine growth retardation during delivery. Soon after birth, he showed phenotypes of suggestive cutis marmorata telangiectatica from the appearance of blood vessels. He had partial syndactyly of the 2nd and 3rd toes, wrinkled palm, and sole skin (Figure 1B). He developed bilateral congenital cataract, hypothyroidism, and partial agenesis of the corpus callosum. The peripheral blood immune profile showed a combined B and T cell immunodeficiencies (Table 1). There were recurrent episodes of bacterial and viral infections. In addition, he showed overall progeria phenotypes and failed to thrive. Patient 1 died at the age of 12 months because of recurrent infections.

3.2 | Clinical presentation of patient 2

Patient 2 was the second child from the same parents, sister of patient 1 (Figure 1A). She showed clinical features that were similar to her brother and included loose saggy skin and seborrheic dermatitis like features. She also had congenital hypothyroidism, bilateral congenital glaucoma and combined B and T cell immunodeficiency. She had similar overall progeria phenotypes along with recurrent bacterial and fungal infections which unfortunately led to her death at the age of 18 months.

3.3 | Identification of nonsense MIC26 variant

We performed whole exome sequencing in both the patients and their parents. There were no major changes except for a point mutation in *APOO/MIC26* (NM_024122.5):c.532G>T (p.E178*) which was inherited from the X chromosome of the mother who is heterozygous for the variant. This variant causes a nonsense mutation that replaces a glutamate with a premature stop codon leading to removal of the last 20 amino acids (Figure 1C). The variant has a minor allele frequency (null) in all the public available databases. We did not find it in any of the more than 200 exomes we analyzed so far on Lebanese patients or healthy individuals. Multiple sequence alignment of MIC26 in various species showed that E178 was conserved among numerous species, while the last 20 amino acids were not as conserved (Figure 1D).

3.4 | MIC26 variant is highly unstable, yet minute amounts of the remaining protein can localize to mitochondria and interact with other MICOS proteins

To determine how MIC26 mutant variant affects the localization and molecular function of MIC26, we generated a plasmid for expression

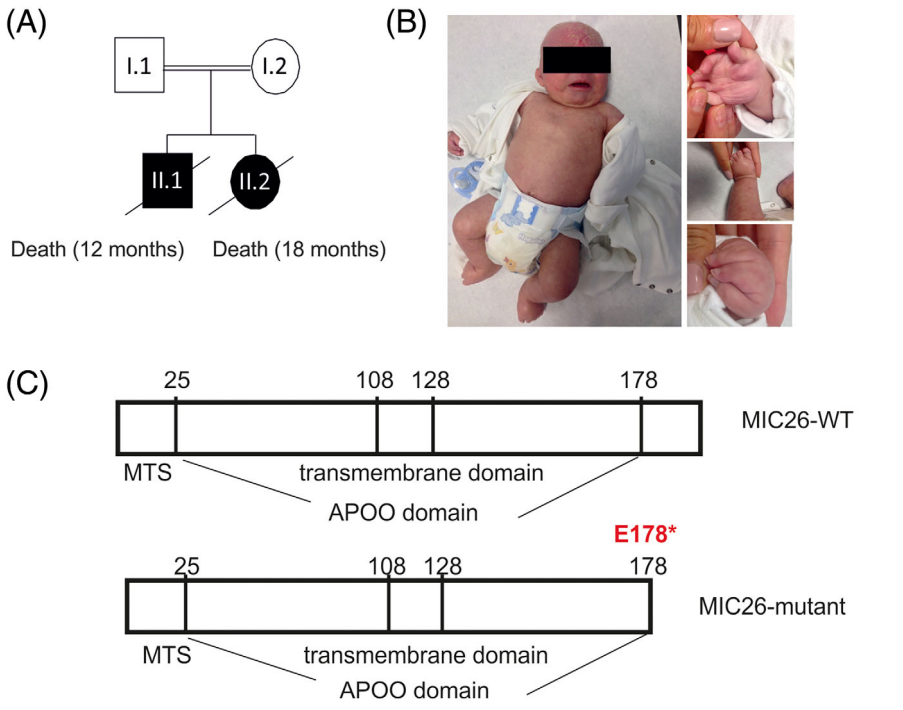

FIGURE 1 A novel missense mutation in *MIC26* causes severe mitochondrial disease with progeria-like symptoms. (A) Pedigree shows that two patients were born in a non-consanguineous marriage. (B) Images of Patient 1 showing symptoms of suggestive cutis marmorata telangiectatica from appearance of blood vessels. Partial syndactyly of the 2nd and 3rd toes, wrinkled palms are shown in insets. (C) Exome sequencing revealed a point mutation in *MIC26* gene which replaces a glutamate (E) at position 178 to a stop codon which causes immature termination and results in a truncated protein lacking last 20 amino acids. (D) Multiple sequence alignment of MIC26 shows that the C-terminal region is not as conserved, however the glutamate E178 is conserved among various species. [Colour figure can be viewed at wileyonlinelibrary.com]

of the human MIC26 mutant variant tagged with GFP, for easy visualization and detection, using site-directed mutagenesis along with WT human *MIC26* gene. MIC26^{WT}-GFP or MIC26^{MUT}-GFP were overexpressed in HeLa cells and visualized using fluorescence confocal microscopy. As expected, MIC26^{WT}-GFP was present in mitochondria shown by co-localization of GFP signal with mitochondrial

TABLE 1 Peripheral blood immune profile of patient 1 showed marked decrease in B-lymphocytes and T-lymphocytes.

Parameter	Percent	Value/absolute count
CD3+	57.39	1403.83
CD3 + CD8+	14.08	344.35
CD3 + CD4+	38.64	945.11
CD3 + CD4 + CD8+	0.19	4.61
CD16 + CD56+	20.00	489.16
CD19+	11.98	293.00
CD45+		2446.10
CD4/CD8 ratio		2.74

Note: Multiple gates on the peripheral blood using CD45 expression reveal a moderate decrease in total CD3 positive T-cell levels (moderate decrease in CD4 positive T-cells and marked decrease in CD8 positive T-cells with CD4/CD8 ratio of 2.74), associated with a marked decrease in total CD19 positive B-cells levels and adequate natural killer cells (CD16 + CD56+) levels.

matrix-targeted mCherry (Mito-mCherry). However, the GFP signal from MIC26^{MUT}-GFP was very low and barely visible (Figure 2A), still upon enhancing the contrast, MIC26^{MUT}-GFP was also found to be localized to mitochondria (Figure 2B). These results indicated that MIC26 variant is somehow unstable, yet small amounts of remaining MIC26 protein can localize to mitochondria. We further checked the steady-state expression levels of MIC26^{MUT}-GFP using western blot analysis and found that the levels of MIC26^{MUT}-GFP were very low compared to MIC26^{WT}-GFP (Figure 2C) implicating that the truncation of last 20 amino acids of MIC26 makes it highly unstable and prone to degradation. As the truncated MIC26 variant could localize to mitochondria, we asked whether it can still interact with other MICOS components and/or can incorporate in the MICOS complex. Co-immunoprecipitation experiments were performed by overexpressing MIC26^{WT}-GFP or MIC26^{MUT}-GFP in HAP1 *MIC26* KO cells using anti-GFP antibody. Large amounts of isolated mitochondria were used as an input in these experiments to overcome the problem of low levels of MIC26 mutant variant. Despite very low expression, we detect that most of the MICOS proteins could be eluted with MIC26 mutant variant indicating the ability of MIC26 variant to interact with MICOS components (Figure 2D). Overall, we conclude that the *MIC26* mutation reported here makes the protein very unstable in such a way that most of the mutant protein is either degraded or lost, however the remaining minute amounts of protein are able to localize to mitochondria and bind to other MICOS components.

3.5 | MIC26 variant shows "loss-of-function" phenotypes similar to *MIC26* knockout

In view of lack of material from the patients, we decided to generate a cell line that exclusively expresses the MIC26 mutant variant and can be used to assess the pathogenic effect of *MIC26* mutation on the cells. For this, we stably expressed untagged MIC26^{WT} or MIC26^{MUT} in the HAP1 *MIC26* KO cells, and named them as control-mimic or patient-mimic cell line respectively for convenience in this manuscript (Figure 3A). The HAP1 WT and *MIC26* KO cells expressing the empty vector (ev) were also generated for comparison as control cells. Western blot analysis shows that MIC26 patient-mimic cells lack the full-length MIC26 protein confirming our previous observation that the MIC26 mutant variant is unstable and mostly degraded (Figure 3A). The steady-state levels of other MICOS proteins remain unaltered except for MIC27 which show higher levels in patient-mimic cell lines as well as in the *MIC26* KO cells (Figure 3A) compared to control cell lines. This can be explained due to the antagonistic regulation between MIC26 and MIC27 as described earlier.[38,40] As MIC26 is virtually absent in patient-mimic cells, the MIC27 levels are increased concomitantly implying that the truncated MIC26 is either not fully functional or not in sufficient amount or both. We previously showed that MIC26 and MIC27 are dispensable for the incorporation of other MICOS subunits into the MICOS complex.[40] This means that the MICOS subcomplexes can be stabilized despite the absence or reduction of MIC26 in patient-mimic cells.

Next, we analyzed the effect of MIC26 mutant mitochondrial ultrastructure and cristae morphology using electron microscopy. Control-mimic cell expressing a wild type version of the MIC26 contained lamellar shaped cristae (Figure 3B). Patient-mimic cells showed highly aberrant cristae structures that were reminiscent of *MIC26* KO cells. These cristae were arranged as stacks as many of them lacked CJs (Figure 3B). Similar cristae structures were seen in *MIC26* KO cells. Usually, mitochondrial fragmentation within a cell is associated with mitochondrial dysfunction and acts as an indicator of mitochondrial stress. We analyzed the mitochondrial morphology in all the cell lines by overexpressing mitochondrially targeted GFP (Mito-GFP) to visualize mitochondria. Patient-mimic cells show highly fragmented mitochondria and the extent of fragmentation was similar to that found in *MIC26* KO cells, indicating that the patient-mimic cells show loss-of-function phenotypes (Figure 3C,D). The levels and assembly of RCCs complexes as analyzed by blue native gel electrophoresis were similar in all the cell lines, indicating no severe defects (Figure S1). Overall, we found that the phenotypes of patient-mimic cells were similar to *MIC26* KO w.r.t., mitochondrial as well as cristae morphology. We conclude that the *MIC26* mutation is a loss-of-function mutation.

4 | DISCUSSION

Here, we report a lethal mitochondrial disease due to a nonsense mutation in *APOO/MIC26* which showed an overall progeria-like phenotypes including suggestive cutis marmorata telangiectatica, wrinkled palms and sole skin. MIC26 is a nuclear-encoded mitochondrial protein involved in maintaining mitochondrial membrane architecture. MIC26 with its orthologous partner MIC27 is required for the formation of CJs, stability of respiratory chain (super) complexes, integrity of F_1F_O ATP synthase complexes and cellular respiration.[40] Aberrant cristae and fragmented mitochondria accumulated in patient-mimic cells,

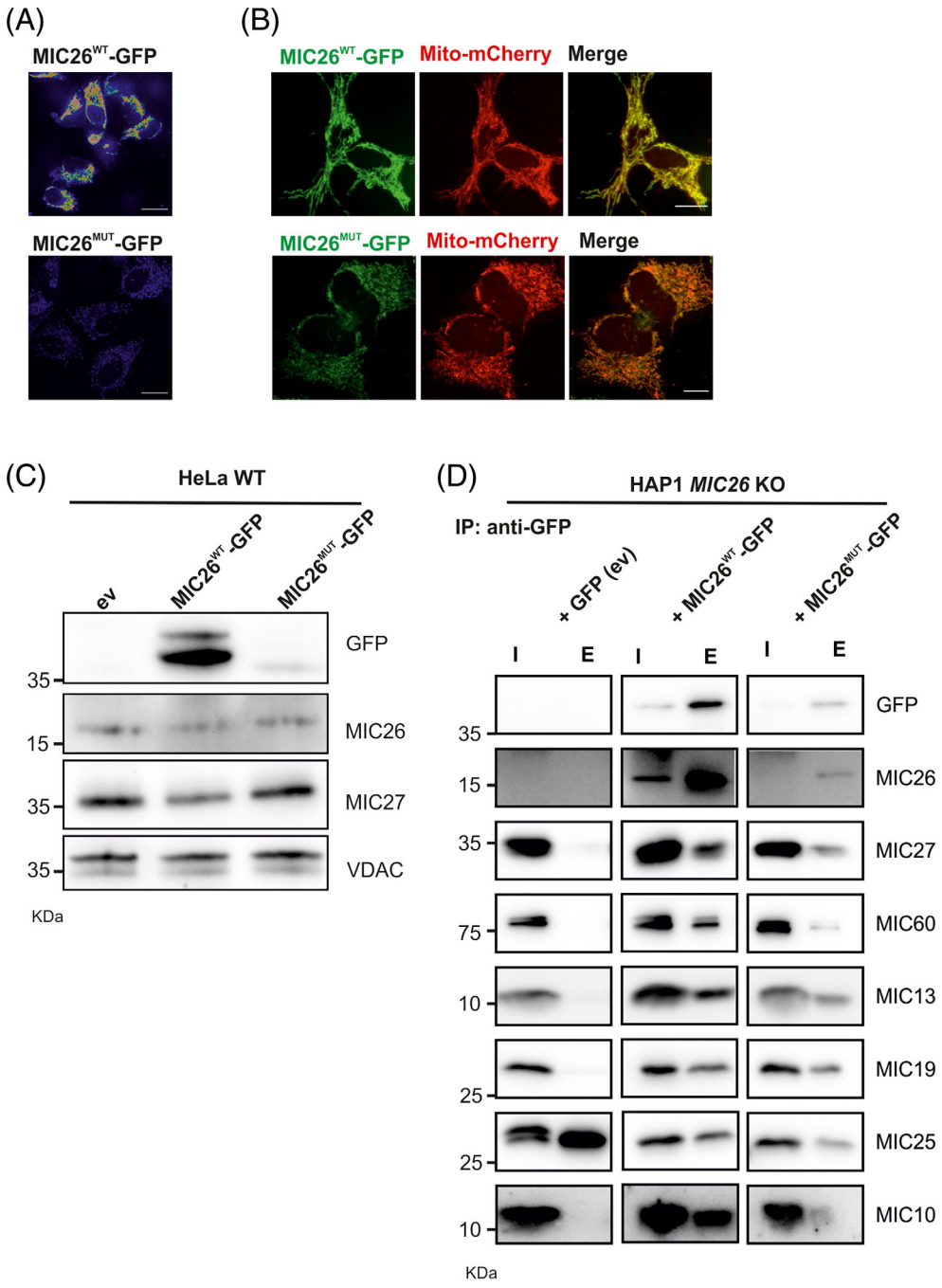

FIGURE 2 Mutant variant of MIC26 is highly unstable and prone to degradation. (A) The images of HeLa cells overexpressing MIC26^{WT}-GFP or MIC26^{MUT}-GFP represented in the rainbow LUT color coding where blue represents very low intensity and red represents high intensity pixels. It shows that the MIC26^{MUT}-GFP has very low expression compared to MIC26^{WT}-GFP. Scale bar 10 µm. (B) HeLa cells overexpressing MIC26^{WT}-GFP or MIC26^{MUT}-GFP were also transfected with mitochondrial-targeted mcherry (Mito-mCherry). MIC26^{WT}-GFP as well as the MIC26^{MUT}-GFP were localized to the mitochondria as shown by colocalization of GFP and mCherry signal. Note that MIC26^{MUT}-GFP was enhanced so that the signal is visible. Scale bar 5 µm. (C) Representative western blots of HeLa cells overexpressing MIC26^{WT}-GFP or MIC26^{MUT}-GFP show that MIC26^{MUT}-GFP was expressed in minute amounts or perhaps unstable. (D) MIC26^{WT}-GFP or MIC26^{MUT}-GFP was expressed in *MIC26* KO and a coimmunoprecipitation (co-IP) was performed using anti-GFP antibody. Huge amounts of mitochondrial samples were taken in these experiments to overcome the problem of very low initial amounts of MIC26^{MUT}-GFP. Despite the low amount of expression, MIC26^{MUT}-GFP could bind to other MICOS components ($N = 3$). [Colour figure can be viewed at wileyonlinelibrary.com]

providing a strong link between mitochondrial function and progression of the observed progeria-like lethal mitochondrial disease. Typical "Progeria" disease known as Hutchinson-Gilford syndrome (HGPA) occurs due to single gene mutation in nuclear gene Lamin A causing aberrant nuclear structure and cell division. Moreover, dysfunctional mitochondria with fragmented morphology, low membrane potential

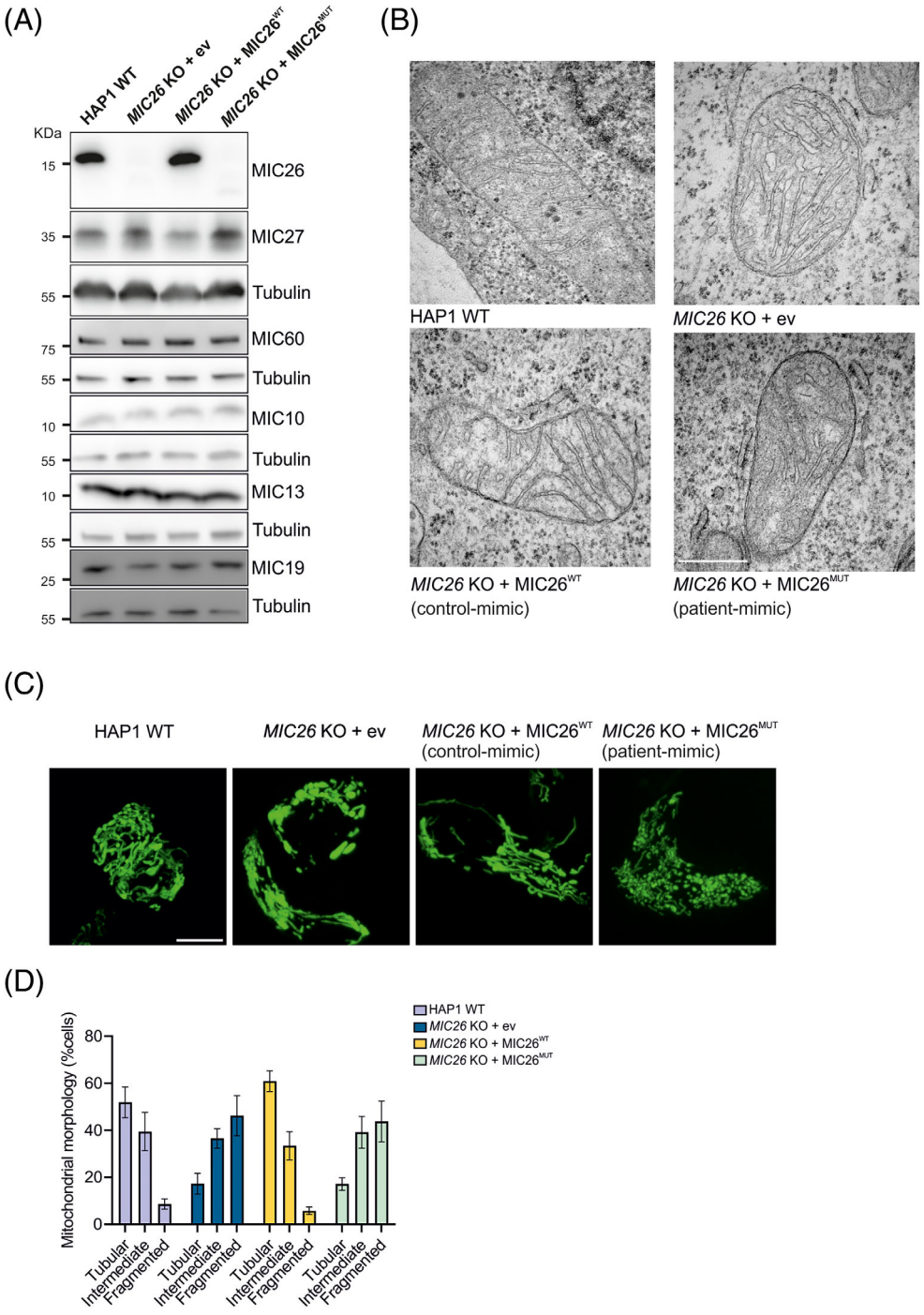

FIGURE 3 *MIC26* mutation behaves as a loss-of-function mutation. (A) Representative western blot for HAP1 WT, *MIC26* KO + ev, *MIC26* KO + MIC26^{WT} (control-mimic), *MIC26* KO + MIC26^{MUT} (patient-mimic) for MICOS proteins. MIC26 is lost in patient-mimic cell lines accompanied by increase in MIC27. This is similar to *MIC26* KO. (B) Representative electron microscopy images of four cell lines, HAP1 WT, *MIC26* KO + ev, *MIC26* KO + MIC26^{WT} (control-mimic), *MIC26* KO + MIC26^{MUT} (patient-mimic). While HAP1 WT and control-mimic cells show normal lamellar cristae structure, perturbed cristae with accumulation of cristae stacks in the mitochondria which lack crista junctions were present in *MIC26* KO + MIC26^{MUT} (patient-mimic) as well as *MIC26* KO cells. (C) Representative images of mitochondrial morphology in the following cells: HAP1 WT, *MIC26* KO + ev, *MIC26* KO + MIC26^{WT} (control-mimic), *MIC26* KO + MIC26^{MUT} (patient-mimic). HAP1 WT and control-mimic cells show normal tubular distribution, but both *MIC26* KO and patient-mimic cells display accumulation of fragmented mitochondria. (D) Bar graph showing the quantification of mitochondrial morphology from three independent experiment ($N = 3$) with each experiment having 40–75 cells from each cell line. [Colour figure can be viewed at wileyonlinelibrary.com]

and respiratory capacity, high ROS levels and low PGC1a levels also accumulated in Progeria.[44,45] Recently, null mutations in Metaxin-2 were found in progeroid disorder mandibuloacral dysplasia.[46] Metaxin-2 and MIC26 are part of a large protein complex called mitochondrial intermembrane space bridge complex (MIB) which help in shaping the mitochondrial cristae. Fibroblasts derived from patients harboring Metaxin-2 null-mutations showed altered nuclear morphology indicating a relationship between mitochondrial function and nuclear stability. This relationship is also reinforced in mutator mouse model which contains mtDNA mutations and shows similar nuclear genome instability as observed in progeric cells.[47]

Surprisingly, the female progeny despite the similar genetic background as her mother manifested a very severe phenotype, while the mother was only a carrier of the mutation. X-linked diseases manifest in males, but very rarely in females as they act as carrier of the variant. This occurs due to a phenomenon of X chromosome dosage compensation, called X inactivation where one of the X-chromosomes is silenced in a random manner to compensate for the differences in number of X chromosome in males and females. However, in very rare cases, a female can manifest a pathogenic variant if their X chromosome inactivation pattern is skewed such that the majority of their normal allele is not expressed. In fact, a study reporting the first *MIC26*

patient mutation also showed such skewed pattern of inheritance in females.[43]

MIC26 is transmembrane protein that resides in the inner membrane which contains a signal sequence, required for import into the mitochondria, and a conserved ApoO domain containing a hydrophobic domain.[38] The *MIC26* mutation occurs due to a single nucleotide mutation that causes the glutamate (E) residue to change to a stop codon leading to premature termination of translation and generation of a truncated protein lacking last 20 amino acids. No specific domain has been assigned to the last 20 amino acids of MIC26 (Figure 1D), however we show that the MIC26 mutant variant which lacks last 20 amino acids is highly unstable indicating faster degradation compared with the WT counterpart. Degradation could possibly take place after import into mitochondria or at the RNA level, however, the mechanism of degradation is not yet investigated. The minute amounts of the remaining MIC26 protein which escaped degradation could localize into mitochondria and also form a complex with other MICOS components. However, it was not sufficient to restore the MIC26 defects and the mutation behaved as a loss-of-function mutation. The previous described mutation in *MIC26* with the variant c.350T>C was shown to induce a missense mutation I117T in the predicted transmembrane domain of MIC26.[43] The mutation caused impaired processing of MIC26 during import and therefore reduced incorporation into the inner membrane. However, overall, the phenotypes of patients were mild with variable range of clinical presentation and severity among the patients that carry this mutation.

MIC26 KO cells as well as patient-mimic cells showed no drastic defect in the levels and assembly of the RCCs. In a previous publication as well, we showed normal RCCs assembly and respiration in *MIC26* KO.[40] Only upon deletion of both *MIC26* and *MIC27*, we found drastic defects in RCCs stability and respiration. Although the scenario could be different in the patient tissues, the general RCCs assembly patterns in cell culture conditions might not reflect the pleiotropic nature of mitochondrial diseases. Differences have been observed in mitochondrial function and activity depending on the kind of sample analyzed, for example, 50% of patients with RCCs defects in muscle biopsies show normal activities in skin fibroblast cultures.[48]

Since its discovery, the importance of MICOS components is growing as more and more pathologies are associated with it. Altered levels of MICOS proteins are associated with human diseases like epilepsy, Down's syndrome, Parkinson's disease, diabetes, and cardiomyopathy.[30] Mutations in *MICOS13/MIC13* cause severe form of mitochondrial encephalopathy with liver dysfunction.[49,50] *IMMT/MIC60* mutations were found in Parkinson's disease patients[51] and mitochondrial developmental encephalopathy with bilateral optic neuropathy.[52] What is surprising is that different proteins as well as different mutations of various MICOS proteins manifest into vastly different phenotypes and syndromes. This shows the importance of mitochondrial membrane structure for proper health and functionality.

AUTHOR CONTRIBUTIONS

Leon Peifer-Weiß: Investigation, methodology, formal analysis, visualization, writing—review and editing. **Mazen Kurban:** Investigation, methodology, data curation, formal analysis, visualization. **Céline David:** Investigation, methodology, formal analysis. **Melissa Lubeck:** Investigation, methodology, formal analysis. **Arun Kumar Kondadi:** Formal analysis, supervision, validation, writing—review and editing. **Georges Nemer:** Conceptualization, data curation, supervision, funding acquisition, investigation, project administration, writing—review and editing. **Andreas S. Reichert:** Conceptualization, supervision, funding acquisition, project administration, writing—review and editing. **Ruchika Anand:** Conceptualization, data curation, formal analysis, supervision, investigation, visualization, methodology, funding acquisition, project administration, writing—original draft, writing—review and editing.

ACKNOWLEDGMENTS

The authors would like to thank Andrea Borchardt and Tanja Portugall for their technical assistance in cloning, electron microscopy, and cell culture. Electron microscopy was performed at the Core facility for electron microscopy (CFEM) at the medical faculty of the Heinrich Heine University Düsseldorf. The research was supported by funding from Medical Faculty of Heinrich Heine University Düsseldorf, Foko-02/2015 (Ruchika Anand and Andreas S. Reichert) and FoKo-2020-71 (Ruchika Anand) and Deutsche Forschungsgemeinschaft (DFG) grants, AN 1440/3-1 (Ruchika Anand), AN 1440/4-1 (Ruchika Anand), KO 6519/1-1 (Arun Kumar Kondadi), and GRK 2576 Vivid (Andreas S. Reichert). Open Access funding enabled and organized by Projekt DEAL.

CONFLICT OF INTEREST STATEMENT

The authors declare no conflict of interest.

PEER REVIEW

The peer review history for this article is available at https://www.webofscience.com/api/gateway/wos/peer-review/10.1111/cge.14420.

DATA AVAILABILITY STATEMENT

The data that support the findings of this study are available from the corresponding author upon reasonable request.

ORCID

Leon Peifer-Weiß https://orcid.org/0000-0002-2391-1937
Mazen Kurban https://orcid.org/0000-0003-1011-0687
Melissa Lubeck https://orcid.org/0000-0002-3935-6552
Arun Kumar Kondadi https://orcid.org/0000-0002-5888-7834
Andreas S. Reichert https://orcid.org/0000-0001-9340-3113
Ruchika Anand https://orcid.org/0000-0001-7337-6007

REFERENCES

1. Vafai SB, Mootha VK. Mitochondrial disorders as windows into an ancient organelle. *Nature*. 2012;491(7424):374-383. doi:10.1038/nature11707
2. Stenton SL, Prokisch H. Genetics of mitochondrial diseases: identifying mutations to help diagnosis. *EBioMedicine*. 2020;56:102784. doi:10.1016/j.ebiom.2020.102784
3. Vogel F, Bornhovd C, Neupert W, Reichert AS. Dynamic subcompartmentalization of the mitochondrial inner membrane. *J Cell Biol*. 2006;175(2):237-247. doi:10.1083/jcb.200605138

4. Wurm CA, Jakobs S. Differential protein distributions define two sub-compartments of the mitochondrial inner membrane in yeast. Research support, non-U.S. Gov't. *FEBS Lett*. 2006;580(24):5628-5634. doi:10.1016/j.febslet.2006.09.012
5. Gilkerson RW, Selker JM, Capaldi RA. The cristal membrane of mitochondria is the principal site of oxidative phosphorylation. *FEBS Lett*. 2003;546(2–3):355-358. doi:10.1016/s0014-5793(03)00633-1
6. Perkins G, Renken C, Martone ME, Young SJ, Ellisman M, Frey T. Electron tomography of neuronal mitochondria: three-dimensional structure and organization of cristae and membrane contacts. *J Struct Biol*. 1997;119(3):260-272. doi:10.1006/jsbi.1997.3885
7. Mannella CA. Structure and dynamics of the mitochondrial inner membrane cristae. *Biochim Biophys Acta*. 2006;1763(5–6):542-548. doi:10.1016/j.bbamcr.2006.04.006
8. Kondadi AK, Anand R, Hansch S, et al. Cristae undergo continuous cycles of membrane remodelling in a MICOS-dependent manner. *EMBO Rep*. 2020;21(3):e49776. doi:10.15252/embr.201949776
9. Huang X, Fan J, Li L, et al. Fast, long-term, super-resolution imaging with hessian structured illumination microscopy. *Nat Biotechnol*. 2018;36:451-459. doi:10.1038/nbt.4115
10. Hu C, Shu L, Huang X, et al. OPA1 and MICOS regulate mitochondrial crista dynamics and formation. *Cell Death Dis*. 2020;11(10):940. doi:10.1038/s41419-020-03152-y
11. Stephan T, Roesch A, Riedel D, Jakobs S. Live-cell STED nanoscopy of mitochondrial cristae. *Sci Rep*. 2019;9(1):12419. doi:10.1038/s41598-019-48838-2
12. Wang C, Taki M, Sato Y, et al. A photostable fluorescent marker for the superresolution live imaging of the dynamic structure of the mitochondrial cristae. *Proc Natl Acad Sci U S A*. 2019;116(32):15817-15822. doi:10.1073/pnas.1905924116
13. Kondadi AK, Anand R, Reichert AS. Cristae membrane dynamics—a paradigm change. *Trends Cell Biol*. 2020;30(12):923-936. doi:10.1016/j.tcb.2020.08.008
14. Harner M, Korner C, Walther D, et al. The mitochondrial contact site complex, a determinant of mitochondrial architecture. Research support, non-U.S. Gov't. *EMBO J*. 2011;30(21):4356-4370. doi:10.1038/emboj.2011.379
15. Hoppins S, Collins SR, Cassidy-Stone A, et al. A mitochondrial-focused genetic interaction map reveals a scaffold-like complex required for inner membrane organization in mitochondria. Research support, N.I.H., extramural research support, non-U.S. Gov't. *J Cell Biol*. 2011;195(2):323-340. doi:10.1083/jcb.201107053
16. von der Malsburg K, Muller JM, Bohnert M, et al. Dual role of mitofilin in mitochondrial membrane organization and protein biogenesis. Research support, non-U.S. Gov't. *Dev Cell*. 2011;21(4):694-707. doi:10.1016/j.devcel.2011.08.026
17. Rabl R, Soubannier V, Scholz R, et al. Formation of cristae and crista junctions in mitochondria depends on antagonism between Fcj1 and Su e/g. *J Cell Biol*. 2009;185(6):1047-1063. doi:10.1083/jcb.200811099
18. Guarani V, McNeill EM, Paulo JA, et al. QIL1 is a novel mitochondrial protein required for MICOS complex stability and cristae morphology. *Elife*. 2015;4. doi:10.7554/eLife.06265
19. Anand R, Strecker V, Urbach J, Wittig I, Reichert AS. Mic13 is essential for formation of crista junctions in mammalian cells. *PloS One*. 2016;11(8):e0160258. doi:10.1371/journal.pone.0160258
20. Urbach J, Kondadi AK, David C, et al. Conserved GxxxG and WN motifs of MIC13 are essential for bridging two MICOS subcomplexes. *Biochim Biophys Acta Biomembr*. 2021;1863(12):183683. doi:10.1016/j.bbamem.2021.183683
21. Stephan T, Brüser C, Deckers M, et al. MICOS assembly controls mitochondrial inner membrane remodeling and crista junction redistribution to mediate cristae formation. *EMBO J*. 2020;39(14):e104105. doi:10.15252/embj.2019104105
22. Tarasenko D, Barbot M, Jans DC, et al. The MICOS component Mic60 displays a conserved membrane-bending activity that is necessary for normal cristae morphology. *J Cell Biol*. 2017;216(4):889-899. doi:10.1083/jcb.201609046
23. Barbot M, Jans DC, Schulz C, et al. Mic10 oligomerizes to bend mitochondrial inner membranes at cristae junctions. *Cell Metab*. 2015;21(5):756-763. doi:10.1016/j.cmet.2015.04.006
24. Hessenberger M, Zerbes RM, Rampelt H, et al. Regulated membrane remodeling by Mic60 controls formation of mitochondrial crista junctions. *Nat Commun*. 2017;8:15258. doi:10.1038/ncomms15258
25. Bock-Bierbaum T, Funck K, Wollweber F, et al. Structural insights into crista junction formation by the Mic60-Mic19 complex. *Sci Adv*. 2022;8(35):eabo4946. doi:10.1126/sciadv.abo4946
26. Ott C, Ross K, Straub S, et al. Sam50 functions in mitochondrial intermembrane space bridging and biogenesis of respiratory complexes. *Mol Cell Biol*. 2012;32(6):1173-1188. doi:10.1128/MCB.06388-11
27. Xie J, Marusich MF, Souda P, Whitelegge J, Capaldi RA. The mitochondrial inner membrane protein mitofilin exists as a complex with SAM50, metaxins 1 and 2, coiled-coil-helix coiled-coil-helix domain-containing protein 3 and 6 and DnaJC11. *FEBS Lett*. 2007;581(18):3545-3549. doi:10.1016/j.febslet.2007.06.052
28. Mukherjee I, Ghosh M, Meinecke M. MICOS and the mitochondrial inner membrane morphology—when things get out of shape. *FEBS Lett*. 2021;595(8):1159-1183. doi:10.1002/1873-3468.14089
29. Anand R, Reichert AS, Kondadi AK. Emerging roles of the MICOS complex in cristae dynamics and biogenesis. *Biology (Basel)*. 2021;10(7). doi:10.3390/biology10070600
30. Eramo MJ, Lisnyak V, Formosa LE, Ryan MT. The 'mitochondrial contact site and cristae organising system' (MICOS) in health and human disease. *J Biochem*. 2020;167(3):243-255. doi:10.1093/jb/mvz111
31. Colina-Tenorio L, Horten P, Pfanner N, Rampelt H. Shaping the mitochondrial inner membrane in health and disease. *J Intern Med*. 2020;287:645-664. doi:10.1111/joim.13031
32. Khosravi S, Harner ME. The MICOS complex, a structural element of mitochondria with versatile functions. *Biol Chem*. 2020;401(6–7):765-778. doi:10.1515/hsz-2020-0103
33. Philip-Couderc P, Smih F, Pelat M, et al. Cardiac transcriptome analysis in obesity-related hypertension. *Hypertension*. 2003;41(3):414-421. doi:10.1161/01.Hyp.0000057573.32425.95
34. Yu BL, Wu CL, Zhao SP. Plasma apolipoprotein O level increased in the patients with acute coronary syndrome. *J Lipid Res*. 2012;53(9):1952-1957. doi:10.1194/jlr.P023028
35. Guo X, Hu J, He G, et al. Loss of APOO (MIC26) aggravates obesity-related whitening of brown adipose tissue via PPARα-mediated functional interplay between mitochondria and peroxisomes. *Metabolism*. 2023;144:155564. doi:10.1016/j.metabol.2023.155564
36. Wu CL, Zhao SP, Yu BL. Microarray analysis provides new insights into the function of apolipoprotein O in HepG2 cell line. *Lipids Health Dis*. 2013;12:186. doi:10.1186/1476-511X-12-186
37. Turkieh A, Caubere C, Barutaut M, et al. Apolipoprotein O is mitochondrial and promotes lipotoxicity in heart. *J Clin Invest*. 2014;124(5):2277-2286. doi:10.1172/JCI74668
38. Koob S, Barrera M, Anand R, Reichert AS. The non-glycosylated isoform of MIC26 is a constituent of the mammalian MICOS complex and promotes formation of crista junctions. *Biochim Biophys Acta*. 2015;1853(7):1551-1563. doi:10.1016/j.bbamcr.2015.03.004
39. Lubeck M, Derkum NH, Naha R, et al. MIC26 and MIC27 are bona fide subunits of the MICOS complex in mitochondria and do not exist as glycosylated apolipoproteins. *PloS One*. 2023;18(6):e0286756. doi:10.1371/journal.pone.0286756
40. Anand R, Kondadi AK, Meisterknecht J, et al. MIC26 and MIC27 cooperate to regulate cardiolipin levels and the landscape of OXPHOS complexes. *Life Sci Alliance*. 2020;3(10):e202000711. doi:10.26508/lsa.202000711
41. Weber TA, Koob S, Heide H, et al. APOOL is a cardiolipin-binding constituent of the Mitofilin/MINOS protein complex determining

cristae morphology in mammalian mitochondria. *PloS One*. 2013;8(5):e63683. doi:10.1371/journal.pone.0063683
42. Rampelt H, Wollweber F, Gerke C, et al. Assembly of the mitochondrial cristae organizer Mic10 is regulated by Mic26-Mic27 antagonism and Cardiolipin. *J Mol Biol*. 2018;430(13):1883-1890. doi:10.1016/j.jmb.2018.04.037
43. Beninca C, Zanette V, Brischigliaro M, et al. Mutation in the MICOS subunit gene APOO (MIC26) associated with an X-linked recessive mitochondrial myopathy, lactic acidosis, cognitive impairment and autistic features. *J Med Genet*. 2021;58(3):155-167. doi:10.1136/jmedgenet-2020-106861
44. Xiong ZM, Choi JY, Wang K, et al. Methylene blue alleviates nuclear and mitochondrial abnormalities in progeria. *Aging Cell*. 2016;15(2):279-290. doi:10.1111/acel.12434
45. Monterrubio-Ledezma F, Navarro-Garcia F, Massieu L, et al. Rescue of mitochondrial function in Hutchinson-Gilford progeria syndrome by the pharmacological modulation of Exportin CRM1. *Cells*. 2023;12(2). doi:10.3390/cells12020275
46. Elouej S, Harhouri K, Le Mao M, et al. Loss of MTX2 causes mandibuloacral dysplasia and links mitochondrial dysfunction to altered nuclear morphology. *Nat Commun*. 2020;11(1):4589. doi:10.1038/s41467-020-18146-9
47. Hamalainen RH, Landoni JC, Ahlqvist KJ, et al. Defects in mtDNA replication challenge nuclear genome stability through nucleotide depletion and provide a unifying mechanism for mouse progerias. *Nat Metab*. 2019;1(10):958-965. doi:10.1038/s42255-019-0120-1
48. Thorburn DR. Practical problems in detecting abnormal mitochondrial function and genomes. *Hum Reprod*. 2000;15(suppl 2):57-67. doi:10.1093/humrep/15.suppl_2.57
49. Russell BE, Whaley KG, Bove KE, et al. Expanding and underscoring the hepato-encephalopathic phenotype of QIL1/MIC13. *Hepatology*. 2019;70(3):1066-1070. doi:10.1002/hep.30627
50. Zeharia A, Friedman JR, Tobar A, et al. Mitochondrial hepato-encephalopathy due to deficiency of QIL1/MIC13 (C19orf70), a MICOS complex subunit. *Eur J Hum Genet*. 2016;24(12):1778-1782. doi:10.1038/ejhg.2016.83
51. Tsai PI, Lin CH, Hsieh CH, et al. PINK1 phosphorylates MIC60/Mitofilin to control structural plasticity of mitochondrial crista junctions. *Mol Cell*. 2018;69(5):744-756. doi:10.1016/j.molcel.2018.01.026
52. Marco-Hernandez AV, Tomas-Vila M, Montoya-Filardi A, et al. Mitochondrial developmental encephalopathy with bilateral optic neuropathy related to homozygous variants in IMMT gene. *Clin Genet*. 2022;101(2):233-241. doi:10.1111/cge.14093

SUPPORTING INFORMATION

Additional supporting information can be found online in the Supporting Information section at the end of this article.

How to cite this article: Peifer-Weiß L, Kurban M, David C, et al. A X-linked nonsense *APOO/MIC26* variant causes a lethal mitochondrial disease with progeria-like phenotypes. *Clinical Genetics*. 2023;104(6):659-668. doi:10.1111/cge.14420